NASA/TM-2011-217162

Methods to Determine the Deformation of the IRVE Hypersonic Inflatable Aerodynamic Decelerator

William R. Young
Langley Research Center, Hampton, Virginia

July 2011

NASA STI Program . . . in Profile

Since its founding, NASA has been dedicated to the advancement of aeronautics and space science. The NASA scientific and technical information (STI) program plays a key part in helping NASA maintain this important role.

The NASA STI program operates under the auspices of the Agency Chief Information Officer. It collects, organizes, provides for archiving, and disseminates NASA's STI. The NASA STI program provides access to the NASA Aeronautics and Space Database and its public interface, the NASA Technical Report Server, thus providing one of the largest collections of aeronautical and space science STI in the world. Results are published in both non-NASA channels and by NASA in the NASA STI Report Series, which includes the following report types:

- TECHNICAL PUBLICATION. Reports of completed research or a major significant phase of research that present the results of NASA programs and include extensive data or theoretical analysis. Includes compilations of significant scientific and technical data and information deemed to be of continuing reference value. NASA counterpart of peer-reviewed formal professional papers, but having less stringent limitations on manuscript length and extent of graphic presentations.

- TECHNICAL MEMORANDUM. Scientific and technical findings that are preliminary or of specialized interest, e.g., quick release reports, working papers, and bibliographies that contain minimal annotation. Does not contain extensive analysis.

- CONTRACTOR REPORT. Scientific and technical findings by NASA-sponsored contractors and grantees.

- CONFERENCE PUBLICATION. Collected papers from scientific and technical conferences, symposia, seminars, or other meetings sponsored or co-sponsored by NASA.

- SPECIAL PUBLICATION. Scientific, technical, or historical information from NASA programs, projects, and missions, often concerned with subjects having substantial public interest.

- TECHNICAL TRANSLATION. English-language translations of foreign scientific and technical material pertinent to NASA's mission.

Specialized services also include creating custom thesauri, building customized databases, and organizing and publishing research results.

For more information about the NASA STI program, see the following:

- Access the NASA STI program home page at *http://www.sti.nasa.gov*

- E-mail your question via the Internet to help@sti.nasa.gov

- Fax your question to the NASA STI Help Desk at 443-757-5803

- Phone the NASA STI Help Desk at 443-757-5802

- Write to:
  NASA STI Help Desk
  NASA Center for AeroSpace Information
  7115 Standard Drive
  Hanover, MD 21076-1320

NASA/TM-2011-217162

Methods to Determine the Deformation of the IRVE Hypersonic Inflatable Aerodynamic Decelerator

William R. Young
Langley Research Center, Hampton, Virginia

National Aeronautics and
Space Administration

Langley Research Center
Hampton, Virginia 23681-2199

July 2011

Available from:

NASA Center for AeroSpace Information
7115 Standard Drive
Hanover, MD 21076-1320
443-757-5802

Table of Contents

Abstract

Small resonant targets used in conjunction with a microwave reflectometer to determine the deformation of the Hypersonic Inflatable Aerodynamic Decelerator (HIAD) during reentry is investigated. The reflectometer measures the distance to the targets and from this the HIAD deformation is determined. The HIAD is used by the Inflatable Reentry Vehicle Experiment (IRVE) which investigates the use of inflatable heat shields for atmospheric reentry. After several different microwave reflectometer systems were analyzed and compared it was determined that the most desirable for this application is the Frequency Doubling Target method.

1. Introduction

The Inflatable Reentry Vehicle Experiment (IRVE) requires a method to measure the deformation and motion of the Hypersonic Inflatable Aerodynamic Decelerator (HIAD) during reentry. It has been proposed that passive resonant targets of the, split ring resonator or other resonator types be placed in strategic locations on the back side of the decelerator next to the heat shield. These targets would be used in a radio frequency continuous wave reflectometry distance measuring system which would frequently (about 100 times per second) measure the distance from the surface antenna mounted on the center column to each target and hence characterize the motion of the IRVE Hypersonic Inflatable Aerodynamic Decelerator. See Figure 1. This approach is simple in concept and requires that a way be found to differentiate or identify each target separately from all other targets. It is believed that target differentiation or identification problems can be solved by using either a resonant target or an active or transponder target. However, it should be noted the active transponder target increases system complexity. This paper attempts to explain the basic principles of radio frequency continuous wave reflectometry and examine several different refinements of this overall approach such as the resonant target and harmonic generating approaches. Examined here are several other candidate approaches with improved target differentiation or identification. Some use active targets.

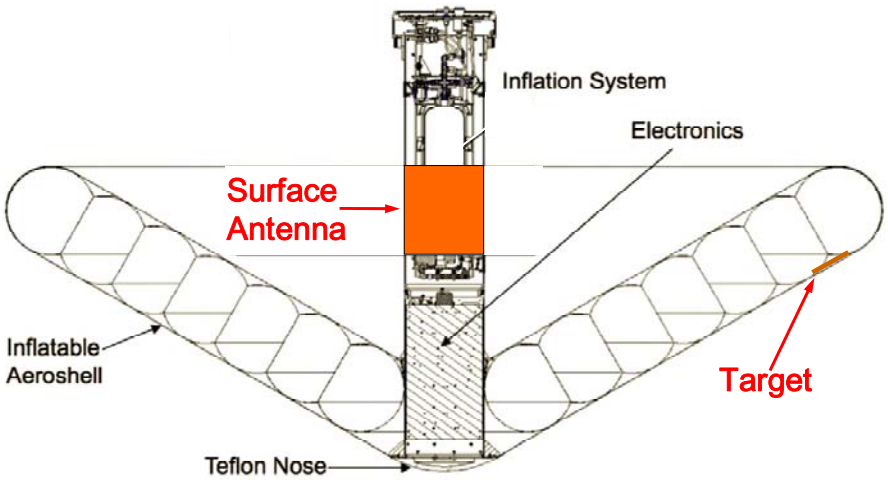

Figure 1. The Hypersonic Inflatable Aerodynamic Decelerator (HIAD)

2. Radio Frequency Reflectometer Distance Measuring System

All of the methods discussed use radio frequency reflectometer distance measurement techniques and measure distance change to the target by determining the phase change of the reflected signal relative to the transmitted signal. To explain or illustrate this, let:

F= frequency of the radio frequency signal used to measure the distance to the target
L =the distance from the transmit antenna to the target.
λ= the wavelength of the signal.
ΔL= the change in distance to the target.
$\Delta \emptyset$= the change in phase corresponding to the change in distance to the target.
C= the speed of light.

The signal travels at the speed of light C; hence λ is given by λ=C/F. Since there are 360 phase degrees in a wavelength, the change in signal path length is related to signal phase change by the ratio 360/λ. For example, if the path length changes by one fourth λ, then the signal phase changes by 90 degrees. The total distance traveled by the radio frequency signal to and from the target is 2L. If the distance to the target changes by ΔL then the path length changes by $2\Delta L$ and the reflected signal phase change relative to the transmitted signal is given by
$\Delta \emptyset = 2\Delta L(360°)/\lambda = \Delta L(720°)/\lambda$.
Solving for the change in distance to the target gives
$\Delta L = \lambda \Delta \emptyset/720°$.
Or in terms of frequency instead of wavelength
$\Delta L = C\Delta \emptyset/720°F$.
Radio frequency reflectometry distance measurement becomes measurement of the change in phase of the reflected signal relative to the transmitted signal.

Ambiguity will result in the determination of ΔL if $\Delta \emptyset$ is equal to or greater than 360 degrees. Knowing the maximum change in L makes it possible to choose a frequency or wavelength which will keep $\Delta \emptyset$ smaller than 360 degrees.

3. Some Methods for Measuring Phase Difference

3.1. The Phase Detector

The phase detector discussed and described here is also known as, and has the same circuit as, a double balanced mixer. Figure 2 shows the circuit configuration of this type phase detector. When used as a phase detector, this three port device or circuit compares two coherent RF signals applied to two of the ports and a voltage proportional to the phase difference between these signals appears at the third port. This output voltage varies sinusoidally with the phase difference between the two RF signals. Figure 3 shows a plot of phase difference between the RF1 and RF2 signals versus a percentage of the maximum output voltage. The region of the sine curve between vertical lines B and C gives an approximate linear relation between phase change and output voltage. This is also true of the sine curve between lines D and E and between lines F and G. These linear regions represent approximately one fourth of a cycle or a 90

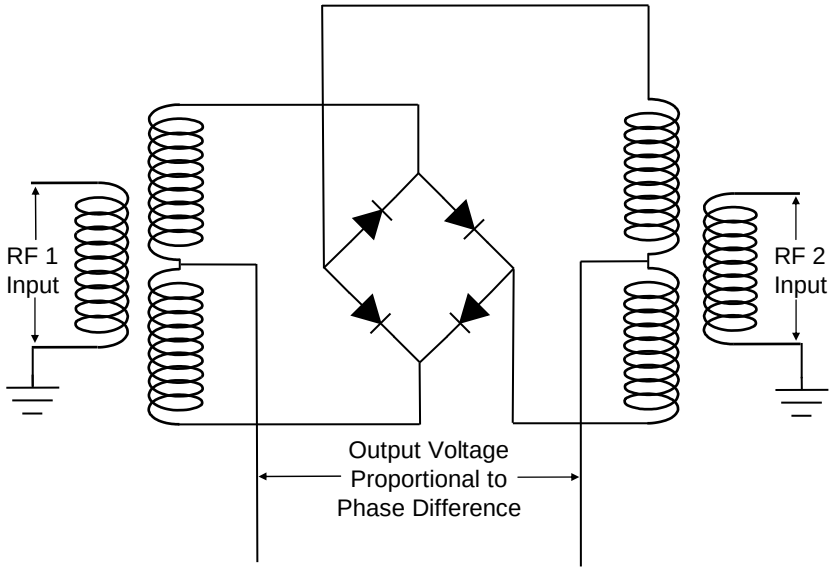

Figure 2. Phase detector circuit.

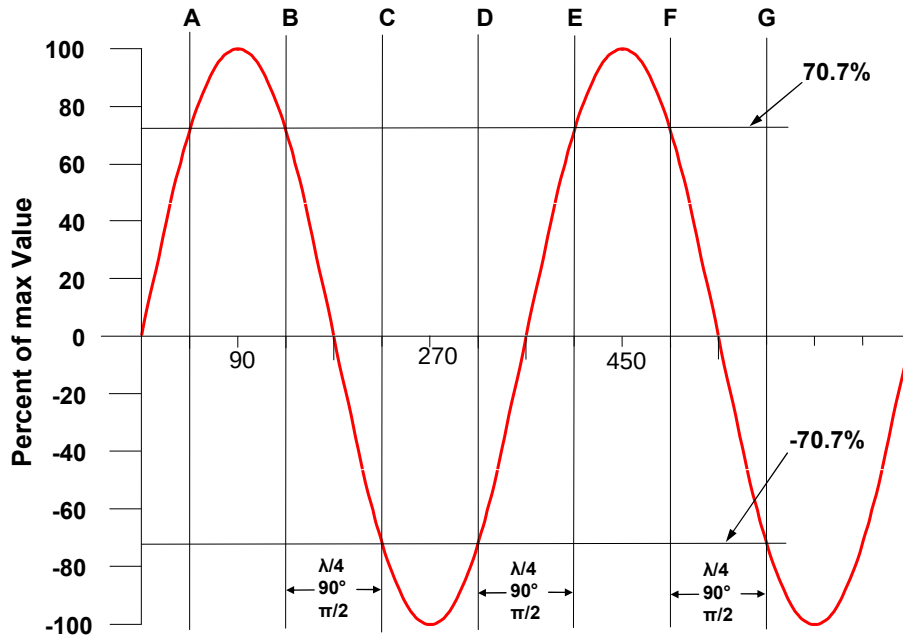

Figure 3. Phase detector output voltage vs phase difference.

degree phase difference. This type of phase detector has an ambiguity problem. Without additional information, it cannot be determined exactly which portion of the sine curve is being indicated. It should also be noted that the maximum phase output voltage is dependent on the amplitude of the weaker of the

two applied RF signals. A way must be found for the two RF inputs to be maintained at constant amplitude for accurate phase measurements. One of the two RF inputs is usually from a reference oscillator and will usually have constant amplitude. A limiting amplifier is often used to keep the other RF signal at constant amplitude [Mini-Circuits].

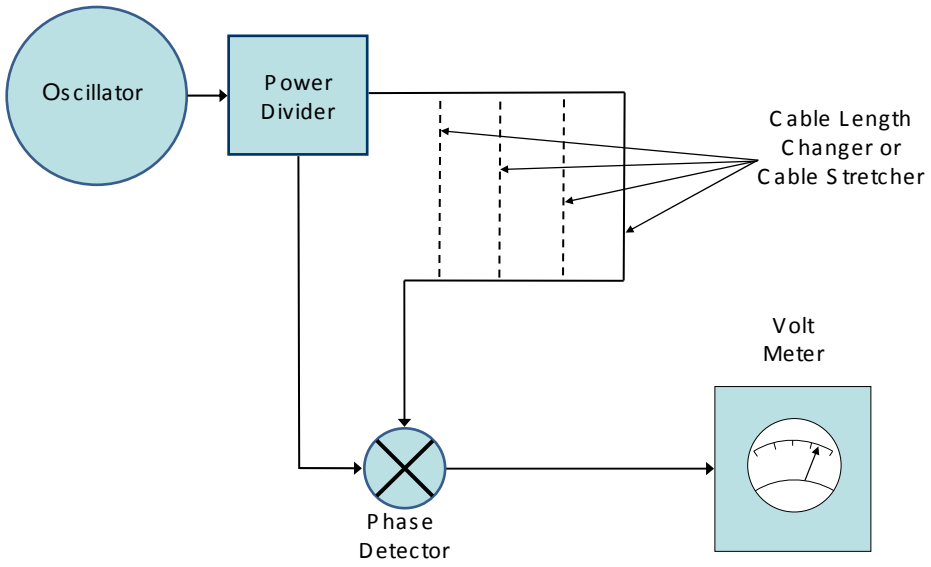

Figure 4. Phase detector demonstration circuit.

Figure 4 shows a block diagram of a phase detector demonstration circuit which uses the phase detector described above. In this arrangement, the signal from the oscillator is divided into two paths by a power divider. In one path the signal is fed directly to the phase detector circuit. The other path goes through a cable length changer, also called a cable stretcher. The cable stretcher changes the physical length of the cable between the power divider and the phase detector. Changing the length of a cable changes the phase at the phase detector port. As explained earlier, increasing the path length by one wave length changes the signal phase by 360 degrees or the phase changes in proportion to the path length change whether in a cable or in free space. The change in output voltage of the phase detector resulting from the phase differences of the two RF input signals is displayed by the volt meter. This output voltage changes as the cable length is changed by the cable stretcher.

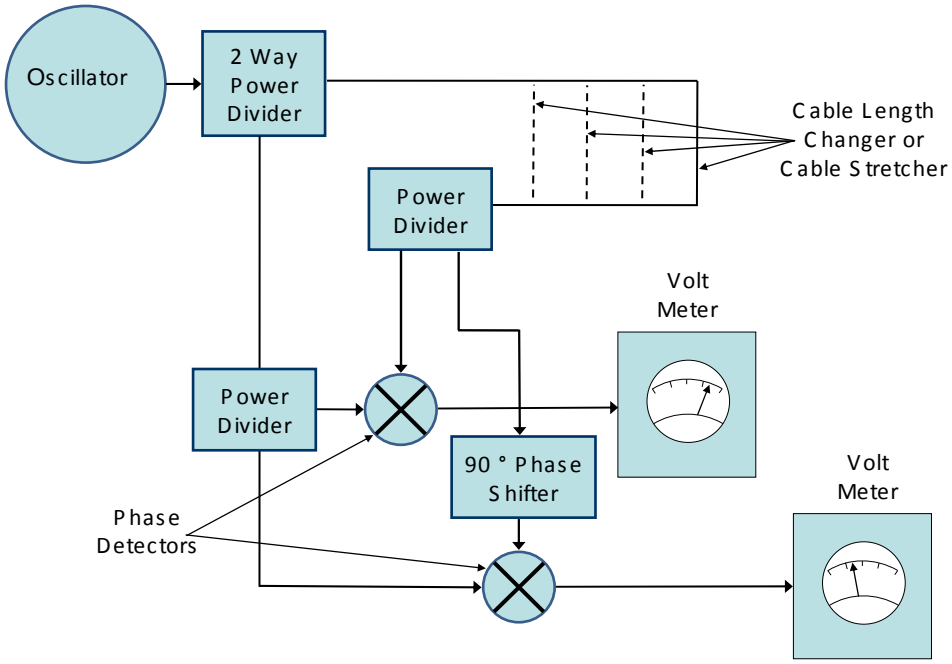

Figure 5. Dual phase detector demonstration circuit.

Figure 5 shows a dual phase detector demonstration circuit which provides a way to eliminate some of the ambiguity with this type phase detector. A second phase detector is added with one of its ports fed by a signal which has had its phase shifted by 90 degrees. The outputs of these two phase detectors are compared in figure 6, where they appear as sine and cosine curves, since shifting a sine curve backward by 90 degrees gives a cosine curve. The top sine curve represents the output of the top phase detector in Figure 5, and the bottom cosine curve represents the output of the bottom phase detector. In Figure 6, notice that between vertical lines A and B the sine curve is nonlinear while the cosine curve is linear. The nearly linear regions are shown in red. Between lines B and C the sine curve is linear while the cosine curve is nonlinear. As we continue from left to right down the sine and cosine curves, notice how the regions of linearity and nonlinearity alternate between curves so that either one or the other is in a linear region. Notice also that when a curve is in a nonlinear region and its polarity is positive, the other curve in the linear region is on a positive slope and vice versa.

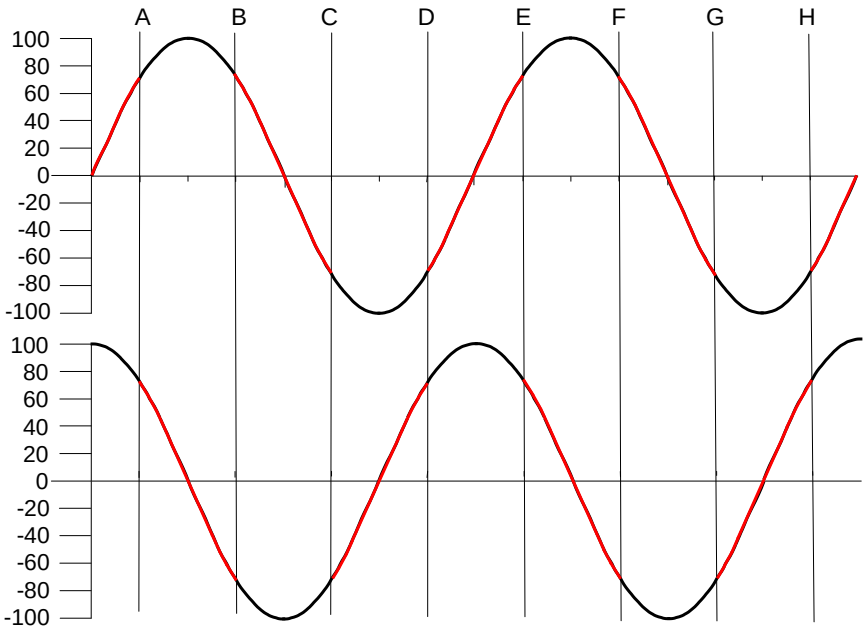

Figure 6. Linear regions of a sine curve.

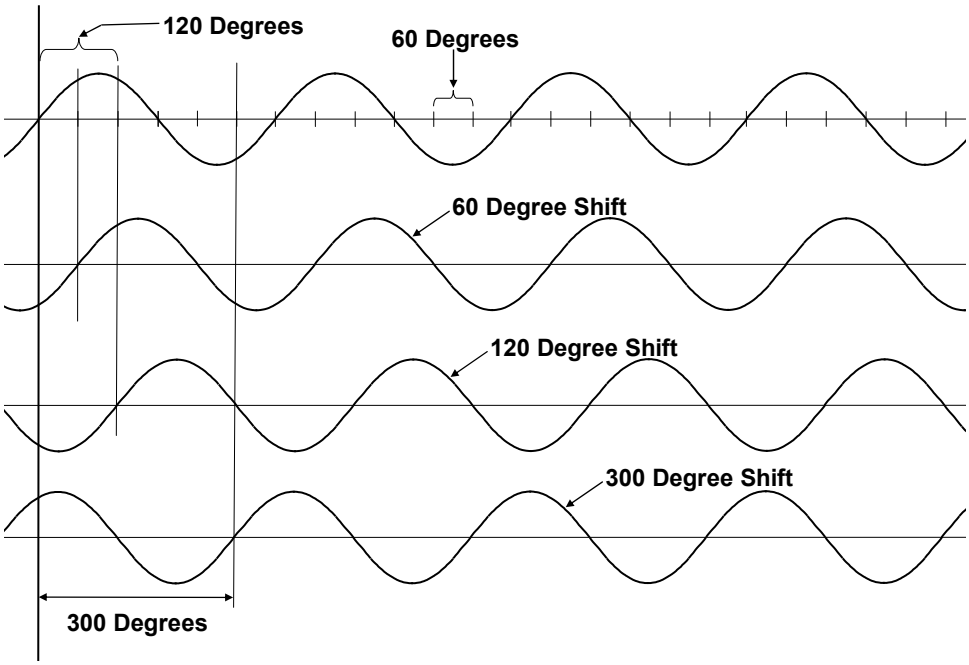

Figure 7. Phase shifted sine waves.

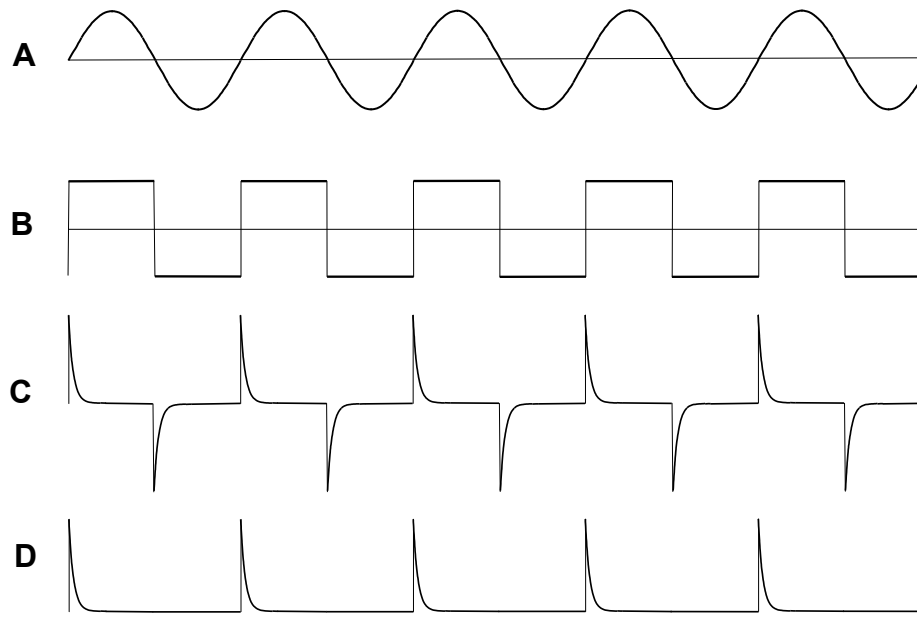

Figure 8. Sine curve zero crossing pulses.

3.2. Phase Determination from Zero Crossings of Sine waves

This method determines the phase difference between the transmitted and reflected signals by measuring the time interval between either the positive going zero crossings or the negative going zero crossings of the sine waves of two RF signals. Figure 7 illustrates how the zero crossings of sine curves relate to phase difference between sine curves. The phase difference is proportional to the time interval between zero crossings.

Amplifying a sine wave in a linear amplifier then clipping its amplitude with a limiter circuit converts the sine wave signal into a square wave. The zero crossing points of the sine and square waves will have the same locations. Converting the sine wave to a square wave does not change the time locations of the zero crossings. This is shown by signals A and B in Figure 8. Passing the square wave through a resistor/capacitor (RC) high pass filter produces a train of narrow pulses shown as C in Figure 8. Each pulse of this pulse train has a sharp leading edge aligned precisely with the zero crossings of the sine wave. Notice the positive going zero crossings of the square wave can be distinguished from negative going zero crossings by the polarity of these pulses. Normally only the positive going pulses are used and the negative going pulses are eliminated from the waveform with a diode clamp circuit, resulting in the pulse train shown as D in Figure 8.

If positive going zero crossing pulse trains are generated for both the reference or transmitted signal and the reflected signal, the positive going pulses of both trains can be compared to find the time between zero crossings of the two signals and from this, the phase difference can be determined. Figure 9 shows a block diagram illustrating two ways to derive phase information from these narrow pulse trains.

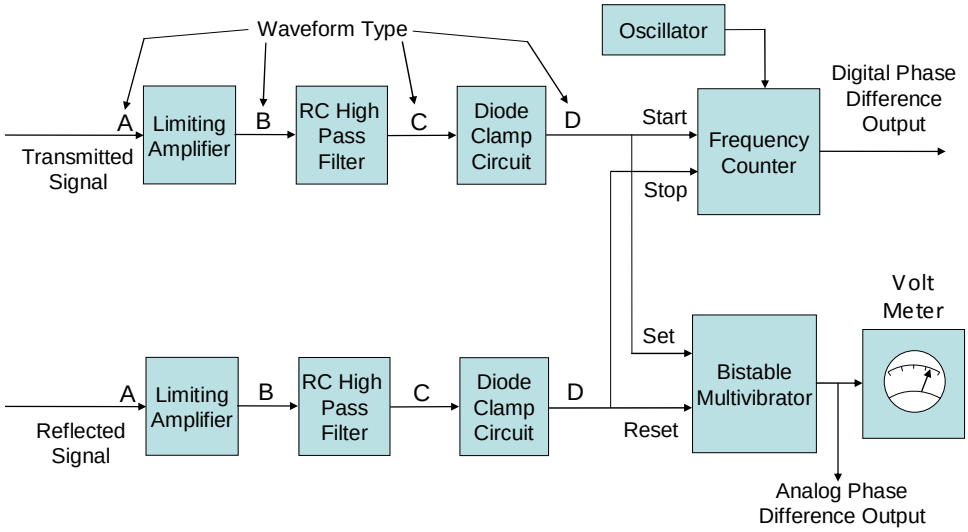

Figure 9. Zero crossing phase detector.

The first method, illustrated in Figure 9 in the top part of the figure, uses a frequency counter the count of which is started by the zero crossing pulse of the reference or transmitted signal. The counter is then stopped and reset by the zero crossing pulse of the reflected signal. This frequency count registered by the counter will be proportional to the phase difference between the signals. Since this data is in digital form, an analogue to digital converter is not required for data downlink.

The second method, illustrated in the bottom part of Figure 9, uses a bistable multivibrator which is set high by the transmitted signal zero crossing pulse and reset to zero by the reflected signal zero crossing pulse. This is illustrated in Figure 10 showing 120 degrees difference between transmitted and received signals. The bottom waveform in the figure shows the output of the bistable multivibrator. Additional signal processing would be required to convert this waveform to an analog voltage which in turn would require an analog to digital converter. Figures 11 and 12 illustrate the 210 degree and the 300 degree cases. Notice that in each case shown in Figures 10 through 12, the output pulse width of the multivibrator is proportional to the phase difference.

The zero crossing phase detector has the advantage of full cycle measurement without ambiguity within the cycle. Again, if the counter output is used to determine the phase, an analog to digital converter is not required.

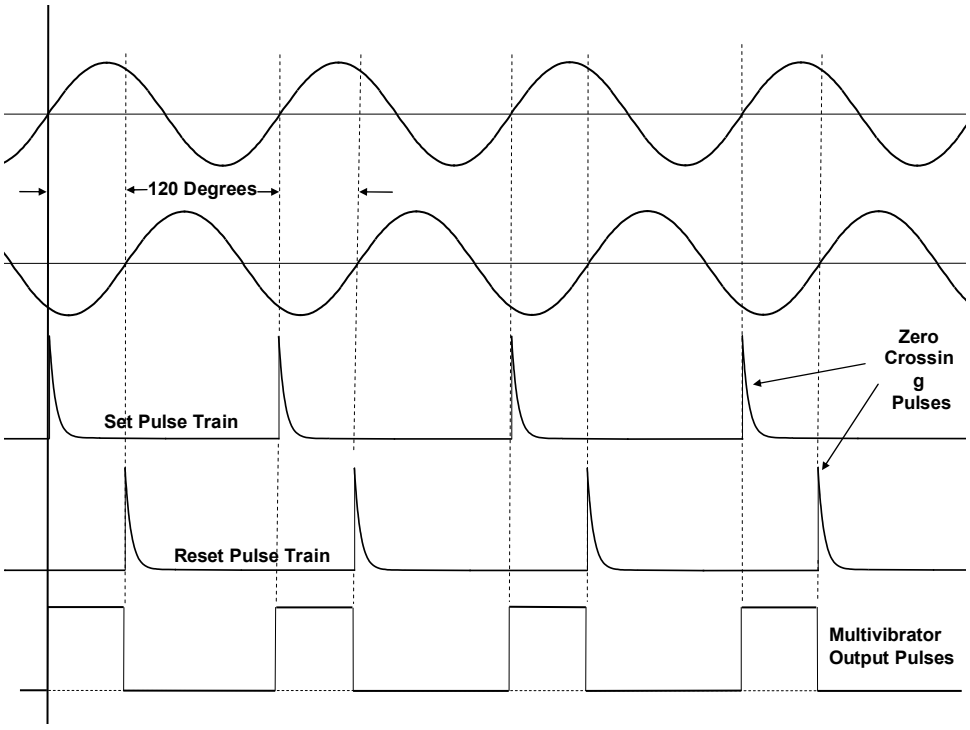

Figure 10. 120 degree analog output pulse train.

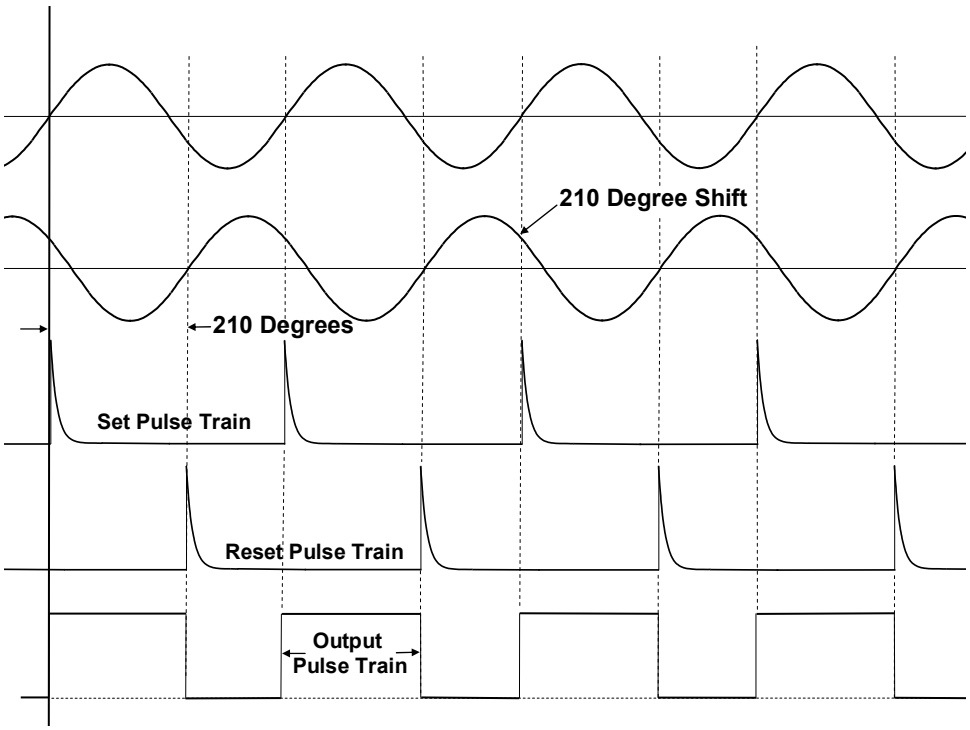

Figure 11. 210 degree analog output pulse train.

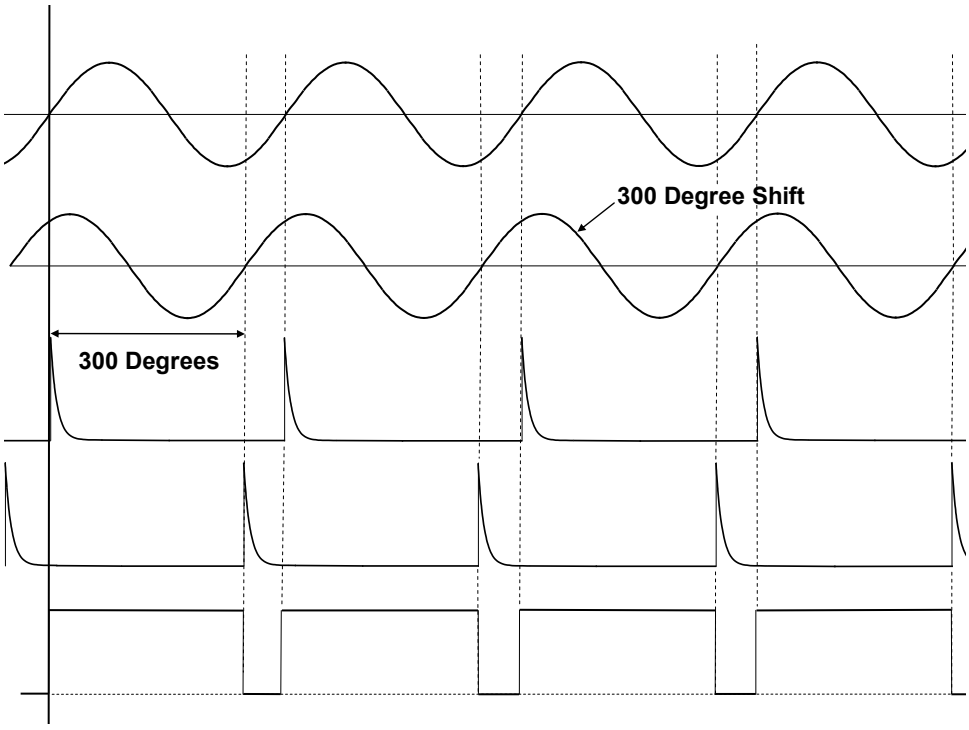

Figure 12. 300 degree analog output pulse train.

3.3. Six Port Probe Method [Bilik]

When a Radio Frequency (RF) signal is reflected from a target, the reflected wave interferes with the incident wave in a manner which depends on the phase of the incident wave when it contacts the target. A "standing wave" is created from the interference between the transmitted wave and the wave reflected. As explained earlier, the source antenna would be located in the center of the HIAD as shown in Figure 1. When a target moves relative to the source antenna the phase of the incident wave at the target changes. This changes the phase relationship between the transmitted and reflected waves causing a positional change in the location of the peaks and valleys of the standing wave. The change in the phase relationship between the transmitted and reflected signals can be determined from this change in the standing wave.

A six port probe can indirectly measure the phase difference between the transmitted and reflected signals by determination of the change in the standing wave pattern. From this change in standing wave the phase change of the reflected wave relative to the transmitted wave is determined. From this change in phase the change in distance to the target is determined. The phase of the transmitted signal is taken as the reference. By measuring the phase change of the reflected signal relative to the phase of the transmitted signal the change in distance to the target can be determined.

The six port probe is a system component with six terminals or ports. Two of the ports are the RF input and output ports. The remaining four ports are connected at sample points inside the device to sample the standing wave in four different locations. From this information the standing wave pattern can be defined mathematically. From the voltages at the four ports, a computer program determines the standing wave pattern from the locations of the peaks and nulls.

4. Some Methods Which Use Phase to Determine Range

4.1. Resonant Targets

Figure 13 shows a block diagram of the configuration envisioned for a reflectometer to measure phase and hence distance to the targets using one of the phase detector circuits discussed above. A directional coupler separates the reflected signal from the transmitted signal, or the directional coupler separates the reflected signal from the standing wave. The reflected signal once separated from the transmitted signal passes through a limiting amplifier. Next it is fed to the phase detector which measures the phase of the reflected signal relative to the transmitted reference signal as previously explained.

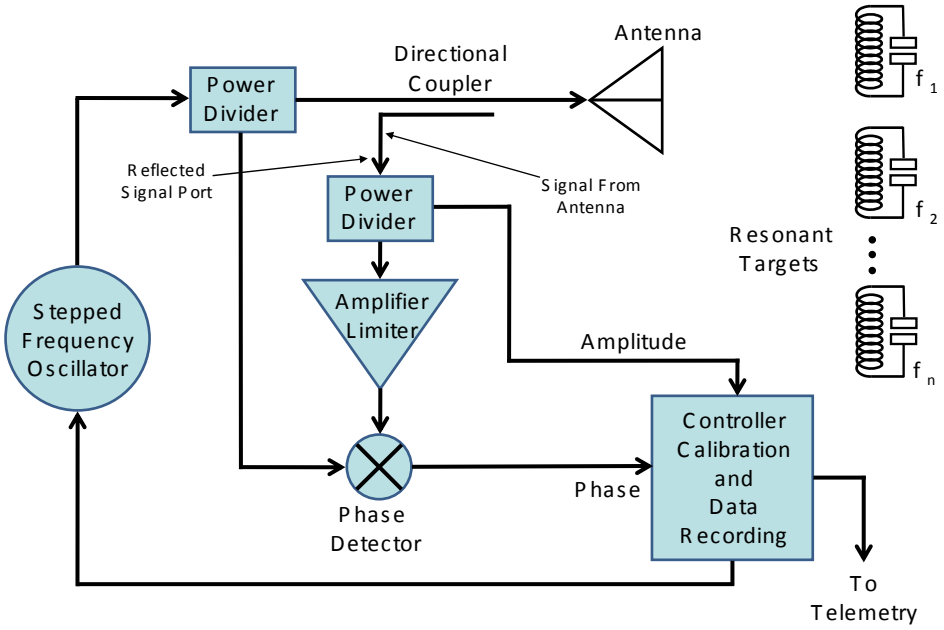

Figure 13. Ranging using a phase detector.

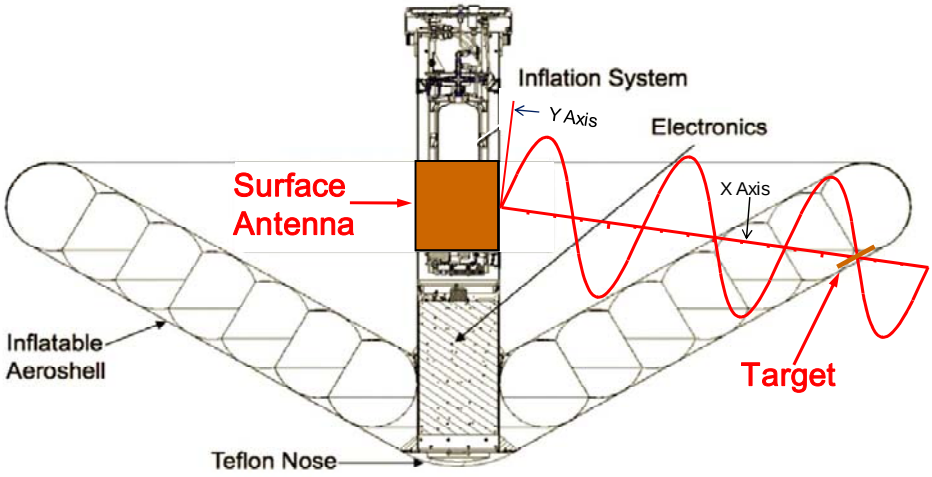

Figure 14. Output voltage change vs target position.

This approach falls in the category of passive resonant targets. Each target is tuned to a different frequency, and reflects more energy when the frequency it receives is at its resonant frequency. A radio frequency signal, generated by a frequency synthesizer, is transmitted from an antenna located in the center of the HIAD to the targets (Figure 1). The frequency synthesizer rapidly steps through the different frequencies of the targets. While the synthesizer is tuned to the frequency of a target, a stronger signal comes from that target than any of the other targets, and this signal is reflected back to the antenna. Here the reflected signal is compared with the transmitted signal and from the change in the phase difference between the transmitted and reflected signals, the change in the distance to the target is determined.

In Figure 14, the red sine wave superimposed on an image of the IRVE Aeroshell illustrates the change in voltage output of the phase detector as a function of target displacement. The target motion along the x axis of the sine wave causes a change in the output voltage of the phase detector. The magnitude of the sine wave (y axis direction) corresponds to the value of the phase detector output voltage caused by the x axis displacement. This voltage is proportional to the phase change.

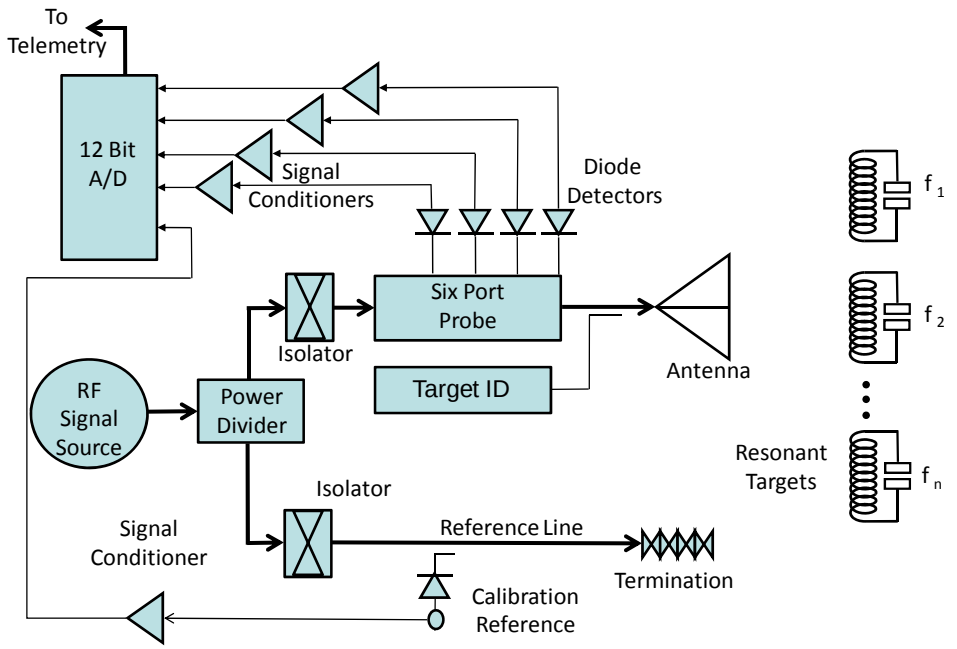

Figure 15. Reflectometer distance measurement using the six port probe.

Figure 15 illustrates one method for measuring range change using the six port probe. In this example resonant targets are again used. This method is similar to the phase detector method described above. As before, a radio frequency signal generated by a frequency synthesizer is used as the signal source. The six port probe does not require that the reflected signal be amplifier limited as is the case with the phase detector. However the six port probe requires computer computations to extract the phase change information from its four diode detector voltage outputs.

4.2. Radio Frequency Identification (RFID)

The targets could incorporate an RFID chip inside to provide target identification. Examples of these systems include Smart Card, "blink", and E-ZPass.

RFID Systems are based on radio frequency (RF) tags and RF readers. These tags contain a microchip with a small memory. Memory capacities of several tens of kilobits or more are possible. RFID systems may be divided in two main categories: passive and active. In passive systems a small antenna receives power from a nearby RF transmitter and captures enough energy to power the logic circuits in the tags. Active systems power the circuits in the tags with batteries, and can support more sophisticated electronics with more data storage capacity, data processing capabilities and / or interfaces to external sensors [Coca].

Having information as to the unique identification of a particular RFID modulated on its return signal carrier does not seem to provide a simple way to distinguish among the different targets [Nititin]. Existing systems can identify only one RFID target in the field at a time. A way must be found to use the subtle difference in the spectrum of each target to determine its unique contribution to the phase change. Multiple RFID transponders responding at once will add to the error vector in much the same way as scattering from nearby structures. This could add to the calibration problem.

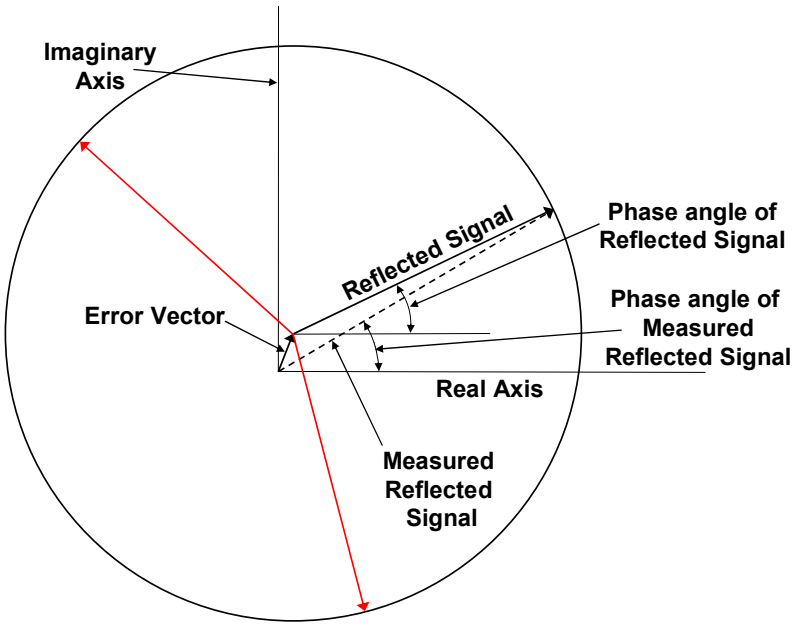

Figure 16. Error vector small relative to the reflected signal vector.

5. Measurement Error Considerations

5.1. The Error Vector

The three phase measuring methods described above are subject to errors which are caused by the imperfections in the system components and the measurement environment. Some examples of these error sources are the antenna mismatch, the directional coupler leakage from the transmitted signal, reflections from objects other than the target (scatter) [Georgiadis], connector mismatch, etc. This is not a complete list of all the possible error sources contributing to the error vector, but these are the largest contributors. All of the individual error sources will add together vectorially and can be thought of as being lumped into a single error vector. Figure 16 shows how this error vector affects the measurement of the actual reflected signal. The real and imaginary axes represent the reference frame from which the amplitude and phase of the reflected signal are actually measured. From Figure 16 we see that the measured phase and amplitude differ from the actual phase and amplitude because of the error vector. Note the circle is centered on the start or tail of the reflected signal vector and not the origin of the coordinate system. This circle represents possible locations or values of the reflected signal vector when the error vector is fixed in both amplitude and phase and the amplitude of the reflected signal is fixed while the phase of the reflected signal is allowed to vary. As the phase of the reflected signal varies through 360 degrees this circle is generated. Actually the amplitude of the reflected signal vector will decrease in magnitude as the target moves away and a spiral rather than a circle would be drawn. To illustrate, two other same amplitude reflected signal vectors, shown in red, are drawn in the circle at different phase angles.

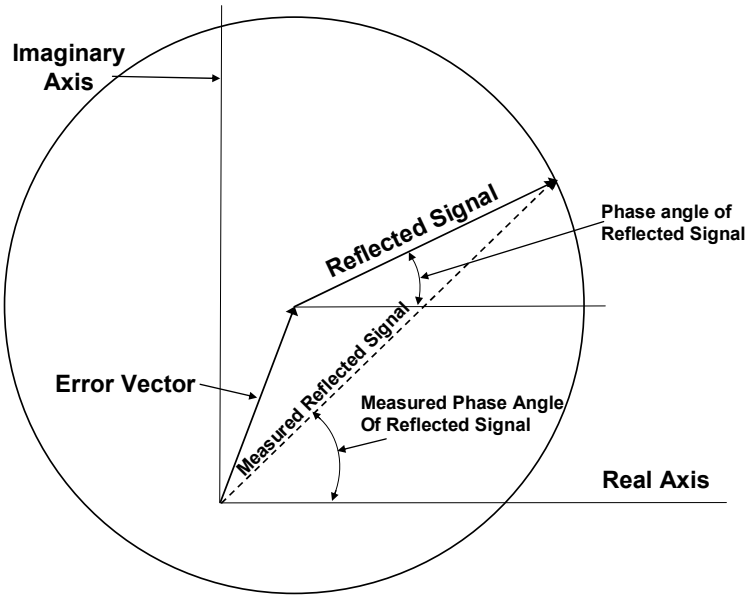

Figure 17. Error vector slightly smaller than reflected signal vector.

Figure 17 shows how as the size of the error vector relative to the size of the reflected signal vector increases, the measured values differ even more from their actual values as would be expected.

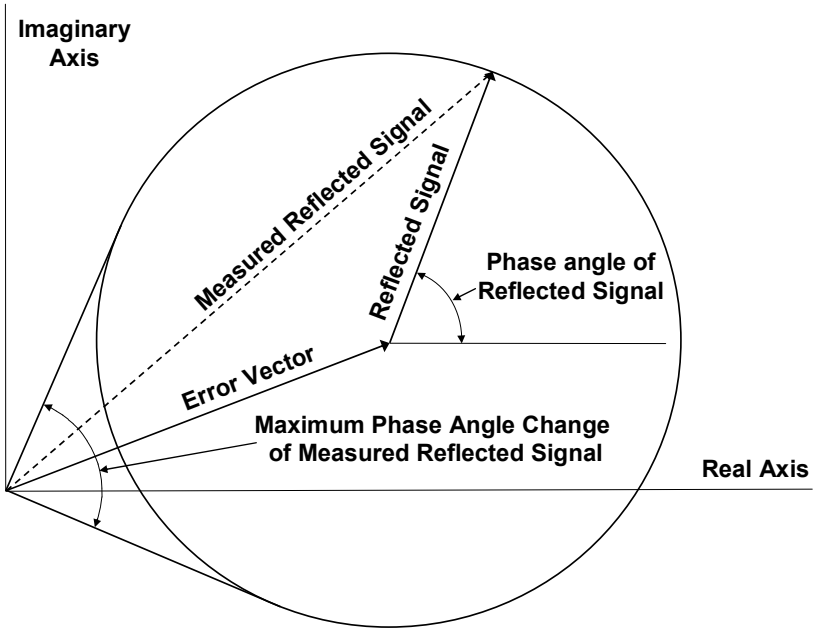

Figure 18. Error vector larger than reflected signal vector.

Figure 18 shows the condition when the error vector is larger than the reflected signal vector. For this case the origin of the coordinate system is outside the circle of the actual reflected signal vector. Notice when this occurs, the possible variation of the measured phase angle of the reflected signal is restricted to a value of less than 360 degrees. For the specific case illustrated in figure 18, the phase change of the reflected signal is limited to a maximum variation of about 90 degrees, while the actual phase angle could vary through a full 360 degrees. From this we see that serious errors can result unless the error vector is considered in the measurement.

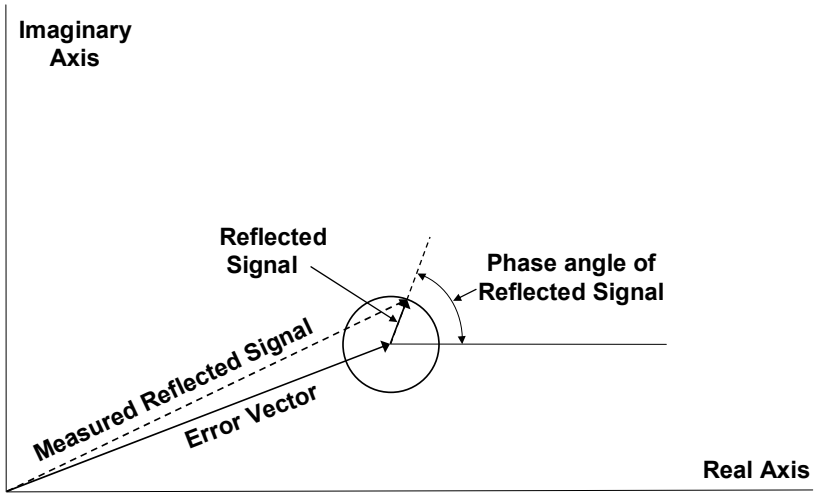

Figure 19. Error vector much larger than reflected signal vector.

Figure 19 shows the condition when the reflected signal is small compared to the error vector. This condition can occur when the return from the target is small perhaps because the range distance is great. From this illustration we can see that as the return from the target gets smaller the measured value for the reflected signal becomes the error vector [Rytting].

Before we can accurately determine the change in distance to the target (range) we must know the phase change of the reflected signal. Before we can know that we must know the magnitude and phase of the error vector. Modern network analyzers have built into their functionality a calibration procedure which measures the error vector associated with each type of measurement. Once determined the error vector is vectorially subtracted from the measured vector to give the desired vector. To accurately determine the range, a way must be found to determine the magnitude and phase of the error vector, a way to minimize it, or both.

5.2. Directional Coupler Leakage

A directional coupler is used in the resonant target method illustrated in Figure 13. Directional coupler leakage of the transmitted signal, antenna connector mismatch and reflections from objects other than the target (scatter), have been identified as the largest contributors to the error vector. Directional coupler leakage and antenna mismatch will be examined as to their contribution to the error vector and their potential to cause problems in determining the error vector and hence the calibration of the reflectometer. Scatter from objects other than the target will not be addressed because at this stage it is an unknown quantity and will probably be much less of a concern.

In Figure 13 note that the signal reflected from the resonant target, which contains the target phase and distance information, is separated from the transmitted signal by the directional coupler located next to the antenna. The reflected signal leaves the directional coupler at its bottom terminal, which we will call the reflected signal port of the directional coupler. From here the reflected signal is fed to a power divider which is the first component of the phase measurement part of this method. It is an unfortunate fact that all directional couplers are imperfect and consequently will let some of the transmitted signal leak into the reflected signal port of the directional coupler. This leaked transmitted signal corrupts the desired reflected signal and introduces an error into the phase measurement. It adds to the error vector.

Directivity is a figure of merit for a directional coupler. The directivity, given in negative dB in the table below, represents a ratio of the transmitted signal leaked into the reflected signal port to the transmitted signal passing through the directional coupler. The higher the directivity or the larger the negative number, the smaller the leakage of the transmit signal into the reflected signal port.

The data in Table 1 below came from three different manufacturer's data sheets and one manufacturer's catalog. The directional couplers listed represent the ones with the best directivity listed for the 2.0 to 4.0 GHz frequency range. Note the best directional coupler found has a directivity of -30 dB.

Table 1. Directivity of Typical Directional Couplers.

Manufacturer	Model# or Series	Frequency Range In GHz	Directivity In dB	Directivity as ratio
MITEQ	CD-202-403-20S-R	2.0 to 4.0	-20	0.01
MECA	780	2.0 to 4.0	-22	0.00631
PULSAR	C30-24-481/7N	2.0 to 4.0	-18	0.01585
HP	797D	2.0 to 4.0	-30	0.0001

Expressing directivity as a ratio we can write

$$\frac{P_l}{P_t} = \eta \qquad (1)$$

where

η = Directivity

P_t = Transmitted signal power at the directional coupler terminal

P_l = Transmitted power leaked into the reflected signal port.

5.3. The Radar Equation

Again referring to Figure 13, the ratio of the received reflected signal power from the targets at the antenna terminal relative to the transmitted signal power at the same antenna terminal, can be calculated using the radar equation which is

$$P_r = \frac{P_t G^2 \lambda^2 \sigma}{(4\pi)^3 R^4} \qquad \textbf{(2)}$$

where

$P_t =$ The transmitted signal power at the antenna terminal

$P_r =$ The received signal power at the antenna terminal

$\lambda =$ The wavelength of the microwave signal used by the radar

$G =$ The gain of the radar antenna for both transmit and receive

$\sigma =$ The effective radar cross section of the target

$R =$ The distance from the antenna to the target.

From the radar equation we see that the ratio of received reflected power to transmitted power at the antenna input connection is given by

$$\frac{P_r}{P_t} = \frac{G^2 \lambda^2 \sigma}{(4\pi)^3 R^4} . \qquad (3)$$

The above equation is used to calculate the ratio of reflected to transmitted power for various target sizes and antenna gains and the results are shown in Table 2 below. The HIAD of the vehicle in question has an inflated diameter of 3 meters. The range, R, to the targets is therefore 1.5 meters. The wavelength used for the calculations corresponded to a frequency of 2 GHz and the effective radar cross section of the target is assumed to be equal to the actual targer area. For convenience, we will call the ratio of received reflected power to transmitted power, as determined by the above equation, the Radar Ratio.

From examining the data in Table 2 notice that the reflected power at the antenna terminal is very small relative to the transmitted power. The last row of Table 2 shows this to be true even for a large target and a high antenna gain factor.

Table 2. Target Size and Antenna Gain Comparisons

Antenna Gain Factor	Target Area in Square Inches	Target Area in Square Centimeters	Target Area in Square Meters	Receive To Transmit Power Ratio	Receive To Transmit Power Ratio in dB
4	1	6.452	0.000645	2.309E-8	-76.366
4	1.5499	10.0	0.001	3.578E-8	-74.463
4	2	12.904	0.00129	4.618E-8	-73.356
4	4	25.808	0.00258	9.236E-8	-70.345
4	5	32.26	0.00323	1.154E-7	-69.376
4	8	51.616	0.00516	1.847E-7	-67.335
6	1	6.452	0.000645	5.195E-8	-72.844
6	1.5499	10.0	0.001	8.052E-8	-70.941
6	2	12.904	0.00129	1.039E-7	-69.834
6	4	25.808	0.00258	2.078E-7	-66.824
6	5	32.26	0.003226	2.598E-7	-65.854
6	8	51.616	0.005162	4.156E-7	-63.813
8	1	6.452	0.000645	9.236E-8	-70.345
8	1.5499	10.0	0.001	1.431E-7	-68.442
8	2	12.904	0.00129	1.847E-7	-67.335
8	4	25.808	0.00258	3.694E-7	-64.325
8	5	32.26	0.00323	4.618E-7	-63.356
8	8	51.616	0.00516	7.388E-7	-61.314

5.4. Ratio of Leaked to Reflected Power

The ratio of leaked transmitted power to reflected power is given by directional coupler directivity divided by the Radar Ratio. This can be shown as follows

$$\frac{\eta}{\frac{P_r}{P_t}} = \frac{\frac{P_l}{P_t}}{\frac{P_r}{P_t}} = \frac{P_l}{P_t}\frac{P_t}{P_r} = \frac{P_l}{P_r} \tag{4}$$

Note that the smaller the directivity ratio the smaller the amount of transmitted power that leaks into the reflected signal port to adversely affect the reflected signal. In Table 1 the best directional coupler listed has a directivity of -30 dB. This value and the above relationship were used to determine the ratio of leaked transmitted power to reflected signal power for various system parameters as tabulated in Table 3.

Most of the information in Table 2 above is repeated below in Table 3. Two columns have been added for the ratio of leaked to reflected power in linear and dB form. The column for target area in square meters was eliminated to make room for the additional information.

Table 3. Comparison of Leaked to Reflected Power.

Antenna Gain Factor	Target Area in Square Inches	Target Area in Square Centimeters	Receive To Transmit Power Ratio	Receive To Transmit Power Ratio in dB	Ratio of Leaked To Reflected Power in dB	Ratio of Leaked To Reflected Power
4	1	6.452	2.309E-8	-76.366	46.366	43311
4	1.5499	10.0	3.578E-8	-74.463	44.463	27944
4	2	12.904	4.618E-8	-73.356	43.356	21656
4	4	25.808	9.236E-8	-70.345	40.345	10828
4	5	32.26	1.154E-7	-69.376	39.376	8662
4	8	51.616	1.847E-7	-67.335	37.335	5414
6	1	6.452	5.195E-8	-72.844	42.844	19249
6	1.5499	10.0	8.052E-8	-70.941	40.941	12420
6	2	12.904	1.039E-7	-69.834	39.834	9625
6	4	25.808	2.078E-7	-66.824	36.824	4812
6	5	32.26	2.598E-7	-65.854	35.854	3850
6	8	51.616	4.156E-7	-63.813	33.813	2406
8	1	6.452	9.236E-8	-70.345	40.345	10828
8	1.5499	10.0	1.431E-7	-68.442	38.442	6986
8	2	12.904	1.847E-7	-67.335	37.335	5414
8	4	25.808	3.694E-7	-64.325	34.325	2707
8	5	32.26	4.618E-7	-63.356	33.356	2166
8	8	51.616	7.388E-7	-61.314	31.314	1353

The ratio of leaked to reflected power varies from 43,311 to 1 as the worst case to 1,353 to 1 for the best case which is found in the bottom row of Table 3. This means that even for the best case the leaked transmitted signal will be over 1,000 times greater than the reflected signal. To recover the reflected signal from the combined leaked signal and reflected signal, it will be necessary to somehow measure the leaked signal with no target present, and subtract this from the combined signals as a system calibration. In this situation the error vector is huge relative to the reflected signal vector. This means finding a small difference between two large numbers which requires great accuracy in both measurements. Calibration of the system will be difficult and suggests that a different approach should be used.

5.5. Connector Mismatch and Scatter

Connector mismatch at the antenna input terminal and at the output of the directional coupler will cause additional transmitted power to be leaked to the reflected signal port. The antenna mismatch and the mismatch at the directional coupler terminal can be analyzed in the same manner. Therefore we will only look at the consequences of antenna mismatch. If we let ρ = the reflection coefficient of the antenna input terminal, S = the resulting standing wave ratio, or SWR, and assume a very good antenna match with an SWR of 1.02:1 we can write

$$\rho = \frac{S-1}{S+1} = \frac{0.02}{2.02} = 0.0099 \qquad (5)$$

The reflected power from the antenna mismatch is given by the relationship

$$P_{rm} = P_t \rho^2 \tag{6}$$

Where

P_{rm} = The power reflected due to the antenna mismatch and

P_t = The transmitted signal power.

$$\frac{P_{rm}}{P_t} = \rho^2 = 0.000098 = 9.8E-5$$

When we compare this value with the receive to transmit power ratios calculated with the radar equation and tabulated in the bottom row of Table 2 and Table 3, we see that the transmitted power reflected because of the antenna mismatch is more than 100 times larger than the reflected signal coming from the target. This mismatch signal adds to the directional coupled transmit power leakage and the size of the error vector. This mismatch signal component would be corrected for or subtracted out in the system calibration as described above.

5.6. Importance of Approximately Equal Amplitude

For proper operation all of the phase measuring devices discussed in this paper require the two phase coherent signals to have nearly the same amplitude. Consider the application shown in Figure 15 which uses a six port probe as the phase measuring device. In this case the phase change is determined from the change in the standing wave pattern. The Radar Ratios listed in Table 2 show how much larger the transmitted signal is than the signal reflected from the targets. This indicates that the standing wave created by the reflected wave as it interferes with the transmitted wave will be difficult to measure and to extract the necessary phase information. The case illustrated on the bottom line of Table 2, is probably the best case (easiest to measure) that can be expected. It shows the reflected signal to be 1,355,000 (1/7.388E-7) times smaller than the transmitted signal. This means the six port probe must extract phase change information from a standing wave pattern with variations which are 0.00007388 percent of the overall wave amplitude.

6. The Method of Choice, Frequency Doubling Target

This approach, as illustrated in Figures 20 and 21, uses a radio frequency reflectometry phase shift distance measuring system. It differs from the other methods in that the target transmits back the second harmonic of the signal it receives. Figure 20 shows a functional block diagram of one of the targets and a drawing of the target configuration. The target has dipole receive and transmit antennas. The received signal is sent to a ceramic lowpass filter which keeps signals intended for other targets (all the other target frequencies) from being doubled in the frequency doubler and leaking back to the target receive antenna where these signals would be transmitted and interfere with other targets. Next it is sent to a frequency doubling circuit followed by a ceramic bandpass filter which is tuned to the second harmonic of the intended received signal for this target. The ceramic filter rejects all other harmonics of the received signal generated in the frequency doubler. The second harmonic is transmitted back to the reflectometer

through another dipole antenna mounted orthogonally to the receive antenna. Figure 21 shows one possible configuration of the reflectometer ranging system for use with the frequency doubling target.

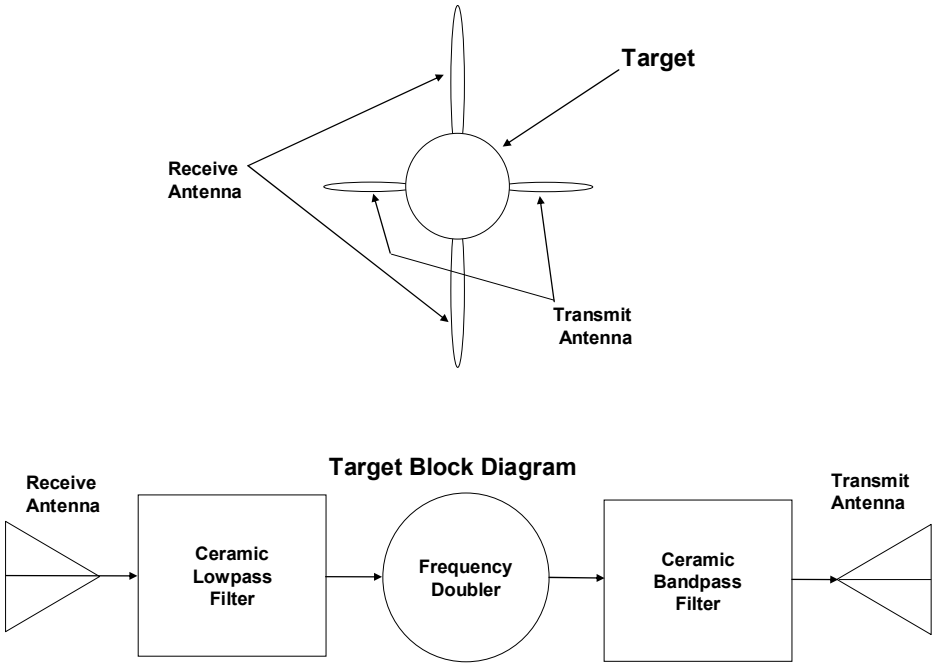

Figure 20. Harmonic generating target.

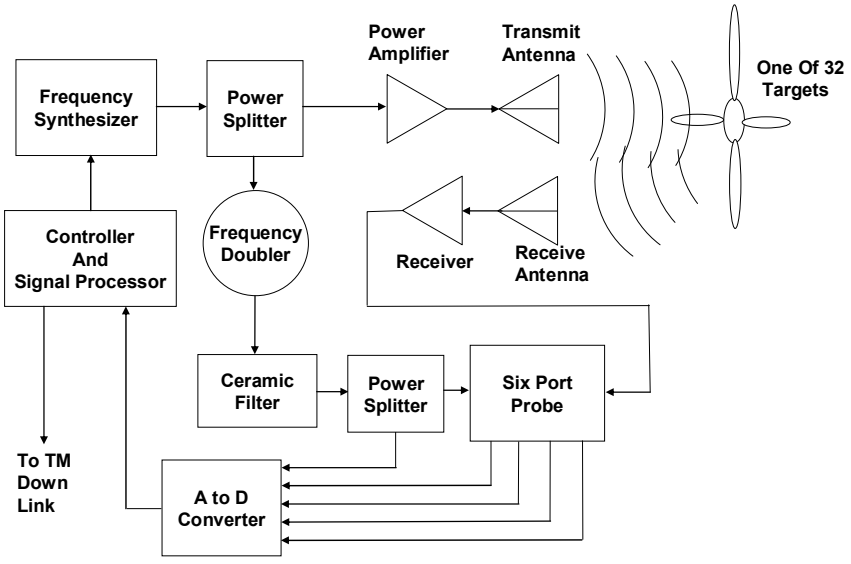

Figure 21. Ranging using harmonic generating target.

Each target has a band pass ceramic filter tuned to a different frequency. Each target's unique ceramic filter frequency enables the system to differentiate between targets because only the target whose frequency matches the frequency being transmitted at that instant will respond with the return of the second harmonic signal. In Figure 21 a harmonic generator like the one in the target generates a reference second harmonic signal in the reflectometer, which is phase coherent with the signal returned from the target. This phase coherent second harmonic reference signal is compared with the signal from the target to get the phase information for range. The controller steps the frequency synthesizer through the frequencies of all the targets in one interrogation cycle.

The Frequency Doubling Target has a distinct advantage over the other ranging methods described here since it is not subject to any of the largest contributors to the error vector. The return signal does not pass through the transmit antenna and a directional coupler is not requited. This eliminates directional coupler leakage, antenna mismatch, and connector mismatch from the list of error sources. Scatter from the transmitted signal will be rejected by the frequency selectivity of the receiver so transmitted signal scatter will be eliminated as an error source also.

A six port probe is shown in Figure 21 as the method for measuring phase difference between the second harmonic of the transmitted signal and the second harmonic signal coming from the target. Note that since the transmitted and received signals are separated from each other it is possible for the received signal to pass through a receiver as shown in Figure 21. The receiver is used to amplify the received signal until it has an amplitude nearly equal to that of the reference signal. When the amplitude of the received signal changes, the automatic gain control of the receiver readjusts the gain so that the received signal is at an optimum level to give maximum accuracy in the phase measurement whether the phase is measured using a six port probe or one of the other methods discussed above.

One source of error unique to the frequency doubling target method is the presence of second harmonics transmitted along with the fundamental frequency. These harmonics are generated by any nonlinearity in the transmit system and will be exactly the same frequency as the signal coming from the harmonic generating target. This signal would be much like the leaked transmitted signal in the directional coupler. The addition of a band pass filter at the transmit antenna will suppress the undesired second harmonic signal and will control this source of error.

Reduced error vector components and frequency selectivity of the targets for improved target identity makes this method the method of choice.

7. Concluding Remarks

As stated above, the Frequency Doubling Target is the method of choice because it is not subject to any of the largest contributors to the error vector. In addition the signal levels applied to the phase detector are at an optimum level for optimum phase detector preformance and accuracy.

The zero crossing phase determination method has the advantages of full cycle measurement without ambiguity within the sine curve cycle. This gives it a clear advantage over the other methods.

It has been implied that only phase needs to be measured to determine the range to the target. In order to determine the error vector and calibrate the measuring system by subtracting the error vector, it will be necessary to measure the amplitude of the measured reflected signal as well. Considerable developmental work will be required to develop a method to determine the error vector and hence calibrate the system.

The operating frequency selection will be influenced by available spectrum and by optimization of the phase slope curve for minimum error while avoiding target position ambiguity. Figures 22, 23, and 24 are plots of frequency versus wavelength. The maximum deflection of the aeroshell should be slightly less than $\lambda/4$**.** This requirement, the plots and the maximum expected aeroshell displacement or deformation make it possible to identify an operating frequency for optimum performance.

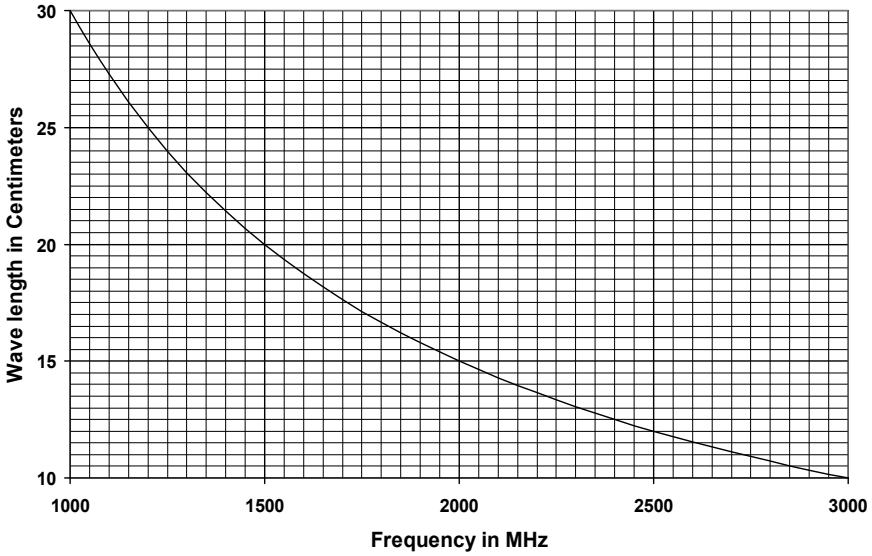

Figure 22. Frequency vs wavelength for lower frequencies.

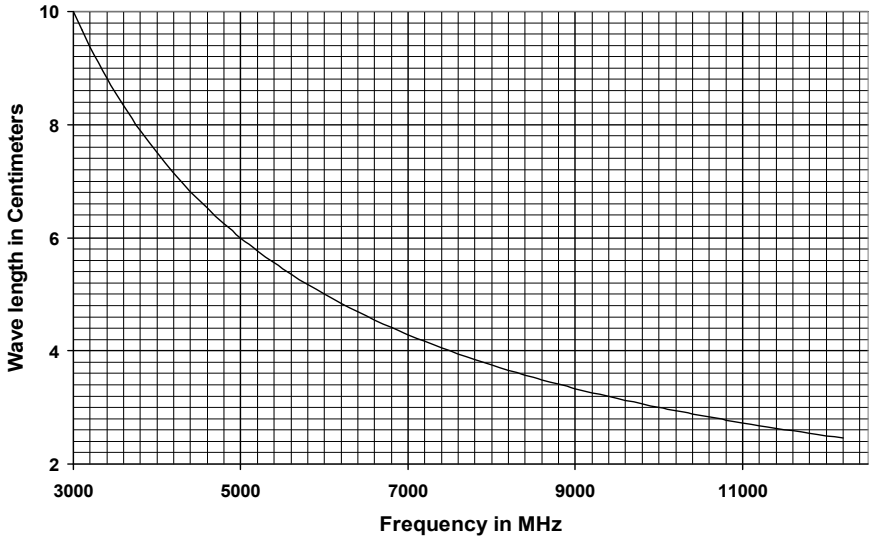

Figure 23. Frequency vs wavelength for higher frequencies.

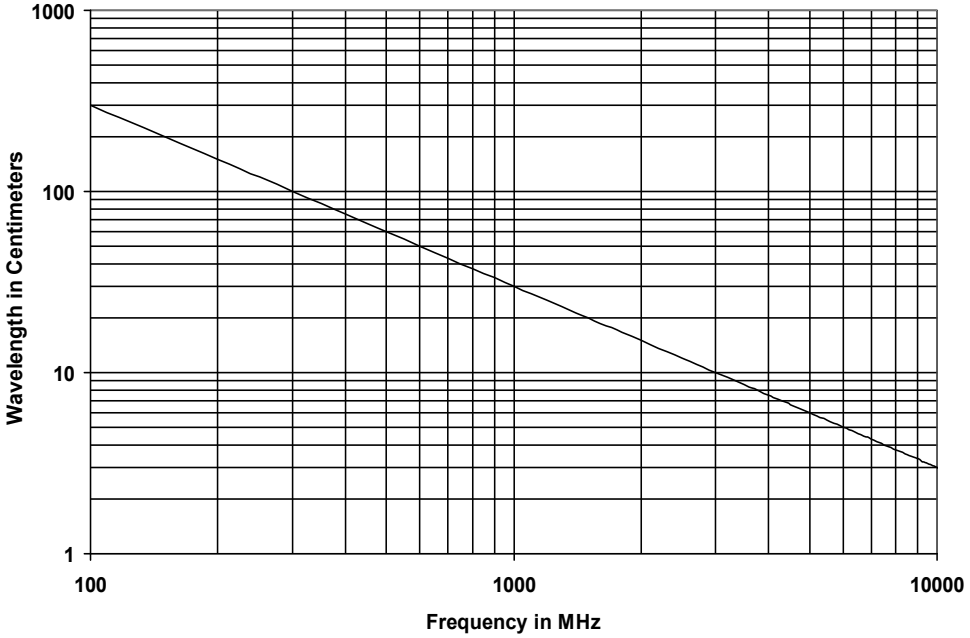

Figure 24. Frequency vs wavelength on logarithmic scale.

References:

[Mini-Circuits] Mini-Circuits Data sheet for model ZRPD-1+Phase Dector Minicircuits.com

[Bilik] Vladimir Bilik, Six-Port Measurement Technique: Principles, Impact, Applications, Slovak University of Technology, Faculty of Electrical Engineering and Information Technology, Ilkovicova 3, SK-81219 Bratislava, Slovakia. E-mail bilikv@elf.stuba.sk

[Coca] Eugen COCA1 , Valentin POPA2, Edvaluation of RFID Location Systrems University "Stefan cel Mare" of Suceava, Faculty of Electrical Engineering and Computer Science, 13, Universitatii Street, 720229, Suceava, Romania, 1eugen.coca@usv.ro, 2valentin.popa@usv.ro

[Nititin] Pavel V. Nikitin, Rene, Martinez, Shashi, Ramamurthy, Hunter, Leland, Gary Spiess, and K. V. S. Rao, Phase Based Spatial Identification of UHF RFID Tags, Intermec Technologies Corporation, 6001 36 th Ave W, Everett, WA, 98203, USA

[Georgiadis] Apostolos Georgiadis, Gain, Phase Imbalance, and Phase Noise Effects on Error Vector Magnitude, IEEE Transactions on Vehicular Technology, Vol. 53, No. 2, March 2004

[Rytting] Douglas Kent Rytting, Network Analyzer Accuracy Overview, Agilent Technologies, 1400 Fountaingrove Parkway, Santa Rosa, CA 95403

REPORT DOCUMENTATION PAGE

Form Approved
OMB No. 0704-0188

1. REPORT DATE *(DD-MM-YYYY)*	2. REPORT TYPE	3. DATES COVERED *(From - To)*
01- 07 - 2011	Technical Memorandum	

4. TITLE AND SUBTITLE

Methods to Determine the Deformation of the IRVE Hypersonic Inflatable Aerodynamic Decelerator

5a. CONTRACT NUMBER

5b. GRANT NUMBER

5c. PROGRAM ELEMENT NUMBER

6. AUTHOR(S)

Young, William R.

5d. PROJECT NUMBER

5e. TASK NUMBER

5f. WORK UNIT NUMBER

737071.01.03.01

7. PERFORMING ORGANIZATION NAME(S) AND ADDRESS(ES)

NASA Langley Research Center
Hampton, VA 23681-2199

8. PERFORMING ORGANIZATION REPORT NUMBER

L-20040

9. SPONSORING/MONITORING AGENCY NAME(S) AND ADDRESS(ES)

National Aeronautics and Space Administration
Washington, DC 20546-0001

10. SPONSOR/MONITOR'S ACRONYM(S)

NASA

11. SPONSOR/MONITOR'S REPORT NUMBER(S)

NASA/TM-2011-217162

12. DISTRIBUTION/AVAILABILITY STATEMENT

Unclassified Unlimited
Subject Category 35
Availability: NASA CASI (443) 757-5802

13. SUPPLEMENTARY NOTES

14. ABSTRACT

Small resonant targets used in conjunction with a microwave reflectometer to determine the deformation of the Hypersonic Inflatable Aerodynamic Decelerator (HIAD) during reentry are investigated. The reflectometer measures the distance to the targets and from this the HIAD deformation is determined. The HIAD is used by the Inflatable Reentry Vehicle Experiment (IRVE) which investigates the use of inflatable heat shields for atmospheric reentry. After several different microwave reflectometer systems were analyzed and compared it was determined that the most desirable for this application is the Frequency Doubling Target method.

15. SUBJECT TERMS

HIAD, IRVE, deformation, microwave, phase, reflectrometry, target

16. SECURITY CLASSIFICATION OF:			17. LIMITATION OF ABSTRACT	18. NUMBER OF PAGES	19a. NAME OF RESPONSIBLE PERSON
a. REPORT	b. ABSTRACT	c. THIS PAGE			STI Help Desk (email: help@sti.nasa.gov)
					19b. TELEPHONE NUMBER *(Include area code)*
U	U	U	UU	33	(443) 757-5802